CHALMERS
UNIVERSITY OF TECHNOLOGY

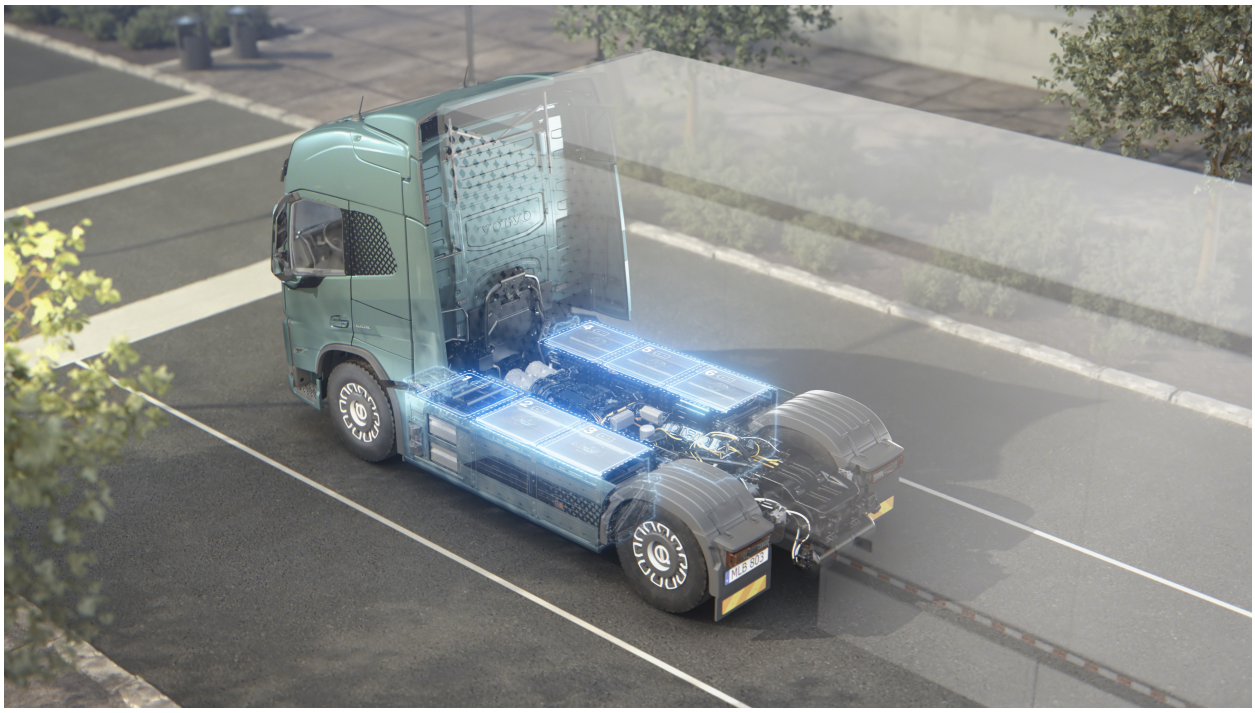

Modeling and Simulation of thermal run-away phenomenons in commercial Li-ion battery cells

Master's thesis in Msc. Mobility Engineering

PRAJWAL SRINIVAS

DEPARTMENT OF MECHANICS AND MARITIME SCIENCES

CHALMERS UNIVERSITY OF TECHNOLOGY
Gothenburg, Sweden 2023
www.chalmers.se

Master's thesis 2023

Modeling and Simulation of thermal runaway phenomenons in commercial Li-ion battery cells

PRAJWAL SRINIVAS

CHALMERS
UNIVERSITY OF TECHNOLOGY

Department of Some Subject or Technology
Mechanics and Maritime Sciences Department
Chalmers University of Technology
Gothenburg, Sweden 2023

Thermal runaway modeling in electric vehicles battery modules
PRAJWAL SRINIVAS

Supervisor: Masih Khoshab, Structural & Thermal Analysis, Volvo Groups
Amirreza Movaghar, Structural & Thermal Analysis, Volvo Groups
Examiner: Dario Maggiolo, Department of Mechanics and Maritime Sciences

Master's Thesis 2023
Department of Mechanics and Maritime Sciences
Chalmers University of Technology
SE-412 96 Gothenburg
Telephone +46 764307033

Cover: Thermal runaway modeling in electric vehicles battery modules.

Typeset in LaTeX
Printed by Chalmers Reproservice
Gothenburg, Sweden 2023

Thermal runaway modeling in electric vehicles battery modules

PRAJWAL SRINIVAS
Department of Mechanics and Maritime Sciences
Chalmers University of Technology

Abstract

Li-ion batteries, while widely adopted, exhibit complex behaviours under extreme conditions that can lead to thermal runaway, a hazardous phenomenon responsible for battery failure and significant safety concerns. The research is motivated by the critical knowledge gaps in the understanding of battery thermal runaway. The limited exploration of the rapid reactions occurring during battery failure, the absence of a specified triggering temperature, and the insufficient understanding of the role of gas formation and gas venting, collectively prompted a deeper investigation. This thesis is focused on gaining a deeper understanding of battery thermal runaway at the cell level. To achieve this, GT-SUITE is utilized to create two models that replicate Accelerating Rate Calorimeter (ARC) battery testing and investigate heat generation and gas venting. The first model combines electrochemical and thermal aspects and analyzes stages of thermal runaway by discretizing them on a cell temperature scale. Such a model not only defines the sequence of events but also calculates the total heat generation for each stage, focusing on the analysis of anode and cathode rapid reactions and their influence on the thermal runaway. The results are validated with experimental results and found to exhibit good accuracy. The second model specifically focuses on gas venting, capturing released gases and analyzing mass loss in the battery cell. Overall, the research presents a detailed analysis of Li-ion battery thermal runaway phenomena while providing temperature and reaction rates boundary conditions for pack-level analysis.

Keywords: Electric vehicles, battery safety, thermal runaway, Li-ion cells, simulation, GT-SUITE, heat, cell venting gas, cell mass loss.

Acknowledgements

The research for the present thesis was done at the Department of Mechanics and Maritime Sciences, at Chalmers University of Technology, Gothenburg, Sweden and Volvo Groups, Gothenburg, Sweden.

I want to extend my sincere gratitude to Masih Khoshab and Amir Movaghar, my supervisors at Volvo Groups, for their continuous support, guidance, and valuable insights throughout this project. Their expertise and recommendations for the project's progression have been incredibly beneficial. I also appreciate their efforts in creating a welcoming atmosphere among the Volvo Group staff.
I also would like to thank my examiner, Professor Dario Maggiolo, for his deep insights and for always being there to provide a hand. His extremely thoughtful act, his prompt email responses, and his insightful criticism motivated me to overcome the difficulties.
My thanks go out to my friends Praveen Raju Hasbavi, Navaneet Subbaram, Yogesh Kumar, and Raju Hurakadalli for their contributions to this thesis.
Lastly, I want to express my heartfelt appreciation to my parents for their unwavering support and care throughout my academic journey, enabling me to complete my Master's program and overcome obstacles.

Prajwal Srinivas, Gothenburg, August, 2023

List of Acronyms

Below is the list of acronyms that have been used throughout this thesis listed in alphabetical order:

BES	Battery Energy Storage
EV	Electric Vehicle
LIB	Lithium-ion battery
BEV	Battery electric vehicle
TR	Thermal Runaway
ISC	Internal Short Circuit
SEI	solid electrolyte interface
NMC	Lithium Nickel Manganese Cobalt Oxide
LFP	Lithium Iron Phosphate
LCO	Lithium cobalt oxide
ARC	Accelerating Rate Calorimetry
GC-MS	Gas Chromatography-Mass Spectrometry
SOC	State of Charge
SOH	State of Health
PVDF	Polyvinylidene fluoride
CMC	Carboxymethyl cellulose
DMC	Dimethyl Carbonate
EMC	Ethyl Methyl Carbonate
EC	Ethylene Carbonate
Ca	Cathode
An	Anode
PE	Polyethylene Membrane
OCV	Open circuit voltage
Li	Lithium
g	Grams
J	Joule

Nomenclature

Below is the nomenclature of indices, sets, parameters, and variables that have been used throughout this thesis.

Indices

m	Model
C	Cathode
A	Anode
c	cell

Paramters

V_m	Voltage of model
U_c	Voltage potential of Cathode
U_A	Voltage potential of Anode
I	Current
R_c	Resistance of battery cell
T	Temperature
K	Reaction rate constant
A	Frequency factor
E_A	Activation energy
SEI_{Decomp}	reaction rate of SEI decomposition

Contents

List of Figures

List of Tables

1

Introduction

1.1 Background

As a result of global warming caused by greenhouse gases, drastic climate changes such as heat waves, extreme weather conditions, and drought have been occurring in recent years and experiencing improper weather seasons. To reduce greenhouse gas emissions, many countries have begun to pursue alternatives to fossil fuels. All the industries and sectors utilising fossil fuels are shifting towards implementing the usage of renewable energy in their operational process.
The increased demand for energy by all industries and domestic usage is a great challenge, as well as ensuring this energy has zero or less carbon-di-oxide emissions. Although renewable energy obtained from solar or wind power is available, a proper energy storage system must be implemented.
The reduction of greenhouse gas emissions from the automotive sector is one of the major concerns in recent times. To reduce emissions and protect the environment, automotive industries are shifting towards manufacturing electric vehicles. The energy storage system used in electric vehicles is lithium-ion batteries (LIBs) which are used for their abilities such as having high energy density, high cycle life, and high efficiency. As the energy storage system gets larger, the complexity and safety concerns rise more. LIBs generate more heat energy during the operation of electrical vehicles and it has to be integrated with good cooling systems thus they need to be properly maintained to avoid hazardous situations. One of the most dangerous and extreme issues with these types of battery systems is Thermal Runaway. The exothermic reactions and the severe increase in the temperature of battery cells lead to catastrophic failures.

1.2 Problem Statement

In the rapid demand for electrical vehicles, more complex technologies and components are being added to the vehicle systems to make battery electric vehicles (BEV) better efficient transport systems. In the process of improving the range of BEVs and adding new features to vehicles, automotive industries are using large energy storage systems (ESS) and are concerned about having better safety systems for them. One of the major concerns is thermal problems in ESS. The temperature has a significant impact on life, performance, and safety, and thus the cost of LI-ion batteries and eventually affordability of Electrical Vehicles.

1.3 Objectives

1. To formulate a 1D thermal model of thermal runaway propagation.
2. To identify the chemical events occurring during the thermal runaway process.
3. Building electrochemical models and integrating them with TR Gt-model.
4. Providing Time sequence map of thermal runaway events.
5. To identify the gases produced during thermal runaway and formulate the total mass of gas and heat generated by it during thermal runaway.

1.4 Deliverables

1. The model mimics the accelerating Rate calorimeter testing of Li-ion battery cell thermal runaway testing.
2. Identifying detailed chemical reactions involved in thermal runaway stages.
3. To carry out a parametric study to understand the influence of various cell components producing venting gas.

1.5 Limitations

- Heat Model
  The results and approach of battery thermal runaway just consider the chemical and thermal parameters. The electrical parameters are not considered for thermal runaway conditions. There is no study done related to cell voltage and resistance in this model.
- Gas Model
  The modeling approach is only focused on capturing the second venting gas (combustion gases). Only major six gases are analyzed in the model and other gases are ignored. Cell mass loss is just calculated using venting gas mass not the actual cell mass during thermal runaway.

1.6 Purpose

The purpose of conducting a thesis on battery thermal runaway is to comprehensively investigate this phenomenon in batteries. The most important purpose of the thesis is to provide analytical solutions and an in-depth understanding of battery thermal runaway which would be implemented in maintaining the safety of the battery and passenger.

2
Theory

In the following sections, the battery cell structure, working, materials, and thermal runaway concept will be explained.

2.1 Lithium-ion Batteries

2.1.1 Working principle of LIB

A Lithium-ion battery works by transferring lithium ions between two electrodes, the cathode, and the anode, through an electrolyte [1]. During charging, the lithium ions move from the cathode to the anode, where they are stored as the battery's energy. At the same time, electrons are released from the cathode and travel through the external circuit to the anode, where they are absorbed, completing the electrical circuit. During discharging, the process is reversed, and the stored lithium ions move back to the cathode, releasing energy and allowing electrons to flow through the external circuit, powering the device. The electrochemical reactions that occur during charging and discharging are reversible, allowing the battery to be charged and discharged repeatedly. The efficiency and performance of the Lithium-ion battery depend on several factors, including the specific cathode and anode materials, the electrolyte composition, and the battery's design and operating conditions.

$$\mathrm{LinC_6 + Lim{-}n(NixCoyAlz)O_2} \underset{\text{discharge}}{\overset{\text{charge}}{\rightleftharpoons}} \mathrm{Li_0C_6 + Lim(NixCoyAlz)O_2} \tag{2.1}$$

2.1.2 Structure of LIB

LIBs consist of two electrodes, a positive (cathode) and a negative (anode). The lithium ions move between the two electrodes when the battery is being charged and discharged. The electrode consists of an active material coated on a metal foil, called a current collector.
The active material of the anode is commonly made of graphite, with a current collector of copper. The current collector and the active material are put together by a binder and polyvinylidene fluoride (PVDF) is commonly used.
movement of ions between the electrodes, an electrolyte is used. Liquid electrolytes consist of a salt, containing ions, that are dissolved in one or multiple solvents.
Because the electric conductivity of the active material is poor, it is common to use an additive to improve its performance. For commercial cells, conductive nanocarbon is often used. Furthermore, the two electrodes are separated by a microporous

material, called a separator. When charging the LIB, the lithium ions move from the metal oxide on the cathode through the electrolyte and are inserted into the anode. Simultaneously, the electrons travel through an external circuit, before arriving at the anode. On discharge, the reverse reactions occur, hence the lithium ions are extracted from the anode and move through the electrolyte and intercalate in the cathode, while the electrons move through the outer circuit and produce the electrical energy of the battery [1]. Consequently, at charging, the cathode is oxidized while the anode is reduced [3]. The mechanism of these reactions is shown in Equations 1 and 2, with LiCoO2 as an example of metal oxide. However, Co can be replaced by other metals.

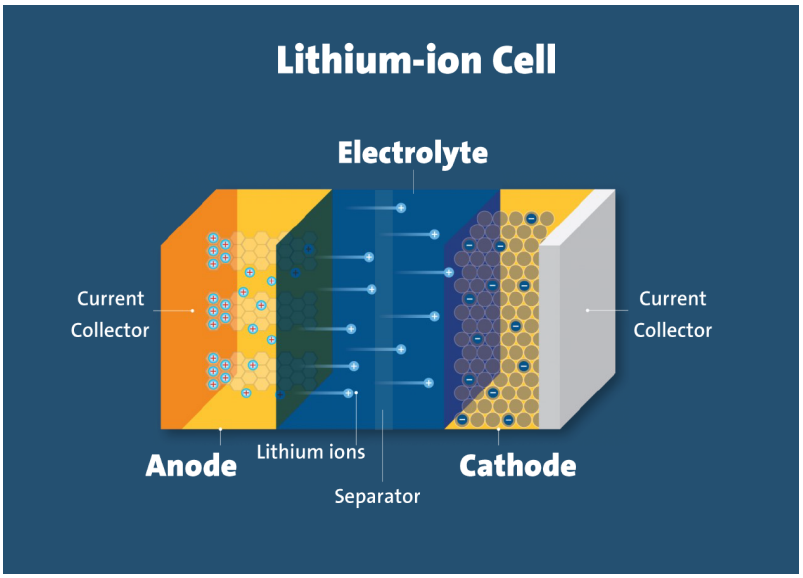

Figure 2.1: Structure of LIB [5]

2.2 Materials of LIB

In this section, the materials of the battery are discussed in detail.

2.2.1 Anode material

The anode is one of the key components in a lithium-ion battery, which is responsible for storing and releasing lithium ions during the charge and discharge cycles [4]. The anode material used in a lithium-ion battery must be able to accommodate the lithium ions as they intercalate into the anode material during charging and then de-intercalate during discharging. Graphite is the most commonly used anode material in lithium-ion batteries, which is an intercalation material. Due to its low cost, high capacity, and stability over many charge and discharge cycles, it is being used as the most common anode material in LIBs. There are other anode materials such as silicon and tin which have high theoretical capacities and could be used for high-performance batteries.
Another structure in the anode is a binder. The binder is an essential component

in the fabrication of anodes in lithium-ion batteries. It is used to hold the active anode material particles together and onto the current collector substrate, such as copper foil or aluminium foil. The binder ensures the anode material stays in place and maintains good electrical contact with the current collector. The most commonly used anode binders are polyvinylidene fluoride (PVDF), carboxymethyl cellulose (CMC), and sodium alginate. The selection of binder materials depends on the requirements of the battery. The chemical reaction of anode in a lithium-ion battery is shown below.

$$\mathrm{nLiC_6} \rightleftharpoons \mathrm{Li_0C_6} + \mathrm{nLi^+} + \mathrm{ne^-} \tag{2.2}$$

2.2.2 Cathode material

The cathode is a key component in a lithium-ion battery, responsible for storing and releasing lithium ions during the charge and discharge cycles. It is typically made of a layered oxide material, such as lithium cobalt oxide (LCO), lithium nickel manganese cobalt oxide (NMC), or lithium iron phosphate (LFP), which provides high specific capacities and excellent cycling stability [6]. The cathode undergoes reduction reactions during charging, in which lithium ions from the electrolyte intercalate into the cathode material and are accompanied by the uptake of electrons from the external circuit. During discharging, the process is reversed, and the cathode releases lithium ions into the electrolyte and releases electrons into the external circuit. The electrochemical properties of the cathode material play a significant role in determining the energy density, power density, and cycle life of the lithium-ion battery. The choice of cathode material depends on several factors, including cost, safety, energy density, and power density requirements of the specific application. Researchers are actively exploring new cathode materials and designs to improve the performance and safety of lithium-ion batteries and enable the development of next-generation energy storage systems.

$$\mathrm{Lim-n(NixCoyAlz)O_2} + \mathrm{nLi^+} + \mathrm{ne^-} \rightleftharpoons \mathrm{Lim(NixCoyAlz)O_2} \tag{2.3}$$

2.2.3 Separator

The separator is a key component in a lithium-ion battery, responsible for keeping the positive and negative electrodes apart while allowing lithium ions to pass through during the charge and discharge cycles. It acts as a physical barrier to prevent direct contact between the cathode and anode, which could lead to short circuits, thermal runaways, and safety hazards. The separator is typically made of a porous polymeric membrane, such as polyethene or polypropylene, with high mechanical strength, good thermal stability, and high electrolyte wettability. The separator must also have a low electrical conductivity to prevent internal short circuits and high ionic conductivity to facilitate the transport of lithium ions. The choice of separator material and design depends on several factors, including the size, shape, and operating conditions of the lithium-ion battery, as well as safety and performance requirements [4]. Researchers are continuously exploring new separator materials and designs to improve the safety, reliability, and energy density of lithium-ion

batteries, and enable their widespread adoption in various applications, including electric vehicles, portable electronics, and grid-scale energy storage

2.2.4 Electrolyte

The electrolyte is a key component in a lithium-ion battery, responsible for conducting lithium ions between the cathode and anode during the charge and discharge cycles. It is typically a solution of lithium salts, such as lithium hexafluorophosphate (LiPF6), lithium perchlorate (LiClO4), or lithium tetrafluoroborate (LiBF4), dissolved in an organic solvent, such as ethylene carbonate (EC), dimethyl carbonate (DMC), or diethyl carbonate (DEC). The electrolyte plays a critical role in determining the performance and safety of lithium-ion batteries, including their energy density, power density, cycle life, and thermal stability. The choice of electrolyte and its composition depends on several factors, including the specific application, battery chemistry, operating conditions, and safety requirements. Researchers are actively exploring new electrolyte materials and formulations to improve the performance and safety of lithium-ion batteries, such as solid-state electrolytes, which offer higher energy density, faster-charging rates, and improved safety compared to conventional liquid electrolytes. The development of advanced electrolyte systems is a key focus of research in the field of energy storage, as it can significantly impact the performance, safety, and cost-effectiveness of lithium-ion batteries, and enable their widespread adoption in various applications.

2.3 Cell Chemistries and its behaviours

2.3.1 Different cell chemistries

- **Lithium Cobalt Oxide(LiCoO2) or LCO:** This is one of the most common cathode materials used in Lithium-ion batteries. It offers high energy density but is sensitive to overheating and has a limited lifespan.
- **Lithium Manganese Oxide (LiMn2O4) or LMO:** This cathode material provides a higher level of safety compared to LiCoO2 batteries. It offers good thermal stability and improved cycle life, although at the expense of slightly lower energy density.
- **Lithium Iron Phosphate (LiFePO4) or LFP:** Known for their enhanced safety characteristics, LiFePO4 batteries have a longer lifespan, better thermal stability, and improved tolerance to high temperatures. They are commonly used in electric vehicles, power tools, and renewable energy storage systems.
- **Lithium Nickel Manganese Cobalt Oxide (LiNiMnCoO2) or NMC:** NMC batteries offer a balance between energy density, power capability, and lifespan. They are widely used in portable electronics, electric vehicles, and grid energy storage applications.
- **Lithium Nickel Cobalt Aluminum Oxide (LiNiCoAlO2 or NCA):** NCA batteries provide high energy density and excellent power performance. They are commonly found in high-end electric vehicles due to their ability to deliver high-power outputs.

- **Lithium Titanate (Li4Ti5O12):** Li4Ti5O12 batteries have excellent cycle life, fast charging capabilities, and good thermal stability. They are often used in applications where high power output and long lifespan are crucial, such as electric buses and energy storage systems.

2.4 Cell Formats

There are several different cell formats for lithium-ion batteries, each with its advantages and disadvantages depending on the specific application. Here are some common formats

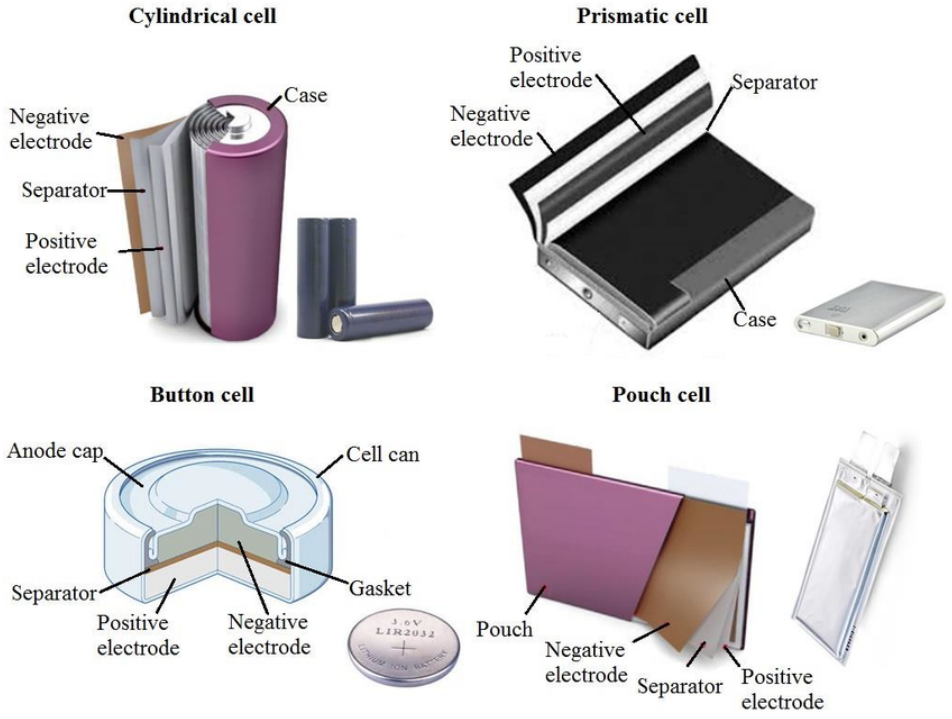

Figure 2.2: Different Cell formats of LIB [7]

2.4.1 Cylindrical cells

Cylindrical cells are the most common format for lithium-ion batteries. They are often used in portable electronics, power tools, and electric vehicles. The cylindrical shape allows for efficient use of space, and the design is easy to manufacture and assemble.

2.4.2 Prismatic cells

Prismatic cells are flat, rectangular cells that are often used in slim, compact devices like smartphones and tablets. They offer a higher energy density than cylindrical cells and can be stacked more efficiently, but their design is more complex and can be more challenging to manufacture.

2.4.3 Pouch cells

Pouch cells are thin, flexible cells that are often used in applications where space and weight are critical, such as wearable devices and drones. They are the lightest and thinnest type of lithium-ion battery, but they require a protective outer casing to prevent damage and can be more expensive to manufacture.

2.4.4 Coin cell

Coin cells are small, flat cells that are often used in applications where small size and low weight are critical, such as smartwatches and hearing aids. They are inexpensive to manufacture, but their small size limits capacity and energy density.

Table 2.1: Comparison of Different Battery Cell Formats

Battery Cell Format	**Shape**	**Size**	**Energy Density**	**Power Density**	**Application**
Cylindrical	Cylindrical	Various sizes	Moderate to high	Moderate to high	Portable electronics, power tools, EVs
Prismatic	Rectangular	Customizable	Moderate to high	Moderate to high	Electric vehicles, energy storage
Pouch	Flexible	Customizable	Moderate to high	Moderate to high	Portable electronics, EVs, drones
Coin	Circular	Small, standardized	Low to moderate	Low to moderate	Watches, calculators, small devices
Large-Format	Various	Large	High	High	Electric vehicles, energy storage
Solid-State	Various	Customizable	High	Moderate to high	Future EVs, portable electronics

The choice of cell format depends on several factors, including the specific application, the required energy and power densities, and the space and weight constraints. Each format has its unique advantages and disadvantages, and researchers are continually exploring new cell designs and materials to improve the performance and safety of lithium-ion batteries.

2.5 Mechanism of thermal runaway

2.5.1 Definition of Thermal runaway

Thermal runaway is a critical phenomenon that can occur in lithium-ion batteries and poses significant safety risks. It refers to a chain reaction of self-heating and escalating temperature within the battery, leading to a rapid and uncontrolled heat release. The mechanism of thermal runaway in lithium-ion batteries involves multiple factors and complex interactions. It typically starts with the occurrence of an

internal short circuit, caused by physical damage, manufacturing defects, or electrode degradation. The short circuit leads to localized high current flow, resulting in localized heating. As the temperature rises, it accelerates the degradation of the battery's components, such as the electrolyte, electrode materials, and separator. This degradation can further increase internal resistance, generating additional heat. The rising temperature can cause thermal decomposition of the electrolyte, resulting in the release of flammable gases and volatile compounds. These gases can then ignite or cause an explosion, exacerbating the thermal runaway process. Understanding the mechanisms behind thermal runaways is crucial for developing safety measures and designing batteries with enhanced thermal management systems to mitigate the risks associated with this phenomenon.

2.5.2 Causes

Abuse conditions can be classified into three categories: mechanical abuse, electrical abuse, and thermal abuse. Mechanical abuse can result in short circuits, which are a recurring element in electrical abuse. A short circuit generates heat and initiates a thermal abuse situation. In a thermal abuse scenario, the battery is subjected to high temperatures, leading to thermal runaway.

- **Mechanical Abuse**: Mechanical abuse typically involves two common characteristics: the destructive alteration and movement resulting from external forces. Instances such as vehicle collisions leading to the crushing or penetration of the battery pack exemplify typical scenarios of mechanical abuse.
  The battery pack deformation is mostly caused in the event of a vehicle collision. This deformation rate depends on the design and arrangement of battery packs in the vehicle. The collision event can lead to hazardous changes in the battery, such as the tearing of the battery separator and the subsequent occurrence of an internal short circuit (ISC), and leakage of the flammable electrolyte, posing a potential risk of fire. The mechanical behaviour of the battery cell mainly depends on the component materials to define the rate of deformation and rupture of internal materials. Modelling of mechanical abuse cases such as during a vehicle collision, penetration is another common occurrence. When penetration happens, it can instantly trigger a powerful internal short circuit (ISC). This means that both mechanical destruction and electrical short-circuiting happen at the same time. The abuse condition of penetration is more severe than simple mechanical or electrical abuse. According to Yamauchi et al. [8], the mechanism of penetration for a cell with a jelly roll was explained. They proposed that in a jelly roll with n sub-cells, each nail creates 2n regions of internal short circuit (ISC). These 2n regions experience a high-level current flow, generating heat following Joule's law. Consequently, the electric energy of the cell is continuously released during the short circuit. The temperature of the cell increases as it absorbs the heat generated by the short circuit. The temperature rise ceases once the cell is fully discharged. If the temperature does not reach a critical level by the end of the short-circuit-induced discharge, no further thermal runaway (TR) will be triggered during

penetration.

- **Electrical Abuse:** An external short circuit occurs when the electrodes, which have a voltage difference, are connected by conductors. The battery pack can experience an external short circuit due to reasons like deformation in a car collision, immersion in water, contact with conductive materials, or electric shock during maintenance. In comparison to penetration, the heat generated by an external short circuit usually doesn't affect the battery cell. There are two major conditions in electrical abuse: overcharge condition, condition in battery thermal runaway, which refers to a situation where a battery is subjected to excessive charging beyond its recommended capacity, leading to severe consequences. The mechanism of overcharge abuse involves the introduction of excessive electrical energy into the battery cell. This excess energy can lead to an uncontrolled chemical reaction and generate substantial heat within the cell. Initially, excessive charging causes an accumulation of lithium ions, which can create metal-like lithium formations. These dendrite formations can penetrate the separator and cause internal short circuits. These short circuits result in a sudden increase in current flow, generating a lot of heat within the battery cell. As the temperature rises, the electrolyte in the battery may break down and release gases like hydrogen. All these events create a dangerous chain reaction. The excessive heat, internal short circuits, and release of flammable gases can cause the battery thermal runaway. Another major electrical abuse condition is the over-discharge condition, in this condition battery thermal runaway occurs when a battery is discharged beyond its recommended limit, leading to the degradation of electrolytes, formation of dendrites, internal short circuits, and potentially hazardous thermal runaway events.

- **Thermal Abuse** Thermal abuse conditions in battery thermal runaway refer to situations where excessive heat is generated within a battery, leading to severe consequences. This can occur due to various factors such as overcharging, over-discharging, exposure to high temperatures, or external factors like fire or heating. During thermal abuse, the temperature within the battery rises rapidly. As the temperature increases, it can cause the electrolyte to degrade and release flammable gases. The pressure inside the battery may also increase, leading to swelling, leakage, or rupture of the battery casing. The elevated temperature can further accelerate chemical reactions, if not controlled, this can result in a thermal runaway event.

As seen in Figure 2.3 it represents the details of battery thermal runaway causes. The ultimate stage of thermal runaway is led by an Internal short circuit. Where the anode and cathode come in contact and the ISC is triggered. It is important to note that not all ISC incidents result in thermal runaway, there are certain cases where we could only observe gas venting during thermal runaway and no fire or explosion is seen. There are also cases where no changes are seen outside of the cell during TR but internal damage of the cell could be detected.

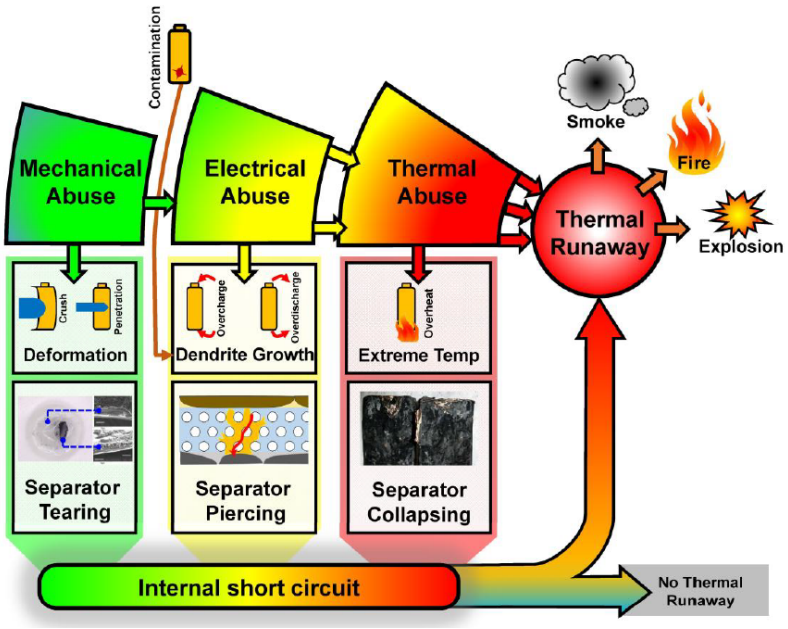

Figure 2.3: Different Causes for Battery thermal runaway [9]

2.6 Stages of Thermal Runaway

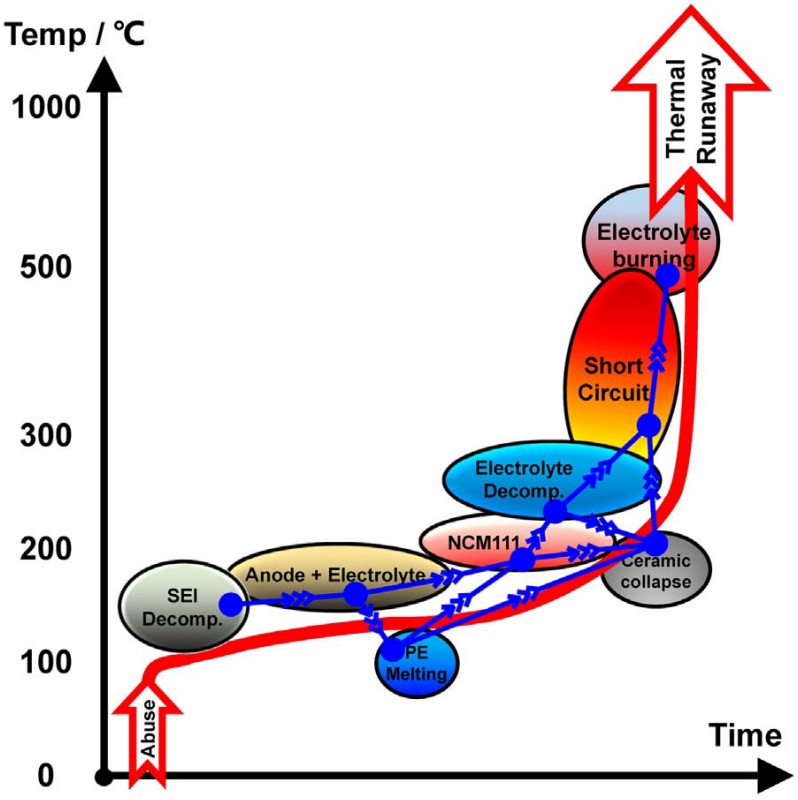

Figure 2.4: Different Stages for Battery thermal runaway [9]

The mechanism of thermal runaway can be understood through a series of chain reactions, as depicted in the figure. Under abusive conditions, once the temperature rises abnormally, chemical reactions occur in a chain-like manner, leading to TR. The Heat-Temperature-Reaction (HTR) loop plays a major role in these chain reactions. Specifically, the abnormal generation of heat elevates the cell's temperature, triggering side reactions such as the decomposition of the solid electrolyte interface (SEI). These side reactions release additional heat, thus forming the HTR loop. The HTR loop continues at extremely high temperatures until the cell experiences TR.

2.6.1 SEI Decomposition

- **SEI Formation**
  The solid electrolyte interface (SEI) layer formation in batteries is a critical process that occurs at the electrode-electrolyte interface. When a battery is first cycled or undergoes initial formation, the SEI layer forms as a result of complex electrochemical reactions. When a battery is initially cycled, electrochemical reactions take place between the electrolyte and electrode surface. These reactions lead to the decomposition of the electrolyte and the generation of reactive species. However, to mitigate these side reactions and improve battery performance, a thin, protective layer known as the SEI layer forms. The SEI layer acts as a physical and chemical barrier between the electrode materials and the electrolyte, preventing direct contact and reducing further degradation. The thickness of a SEI layer may vary from a few tens to hundreds of nanometers. The chemical reactions for the formation of SEI are shown below. The stable operating temperature of the SEI layer is around 0°C to 60°C. This temperature range covers a broad spectrum of ambient conditions encountered in everyday applications.

$$C_3H_4O_3(EC) + 2\,e^- + 2\,Li^+ \longrightarrow (CH_2OCO_2Li)_2 + C_2H_4$$

Electrolyte + Electrode Materials — **Solid Electrolyte Interface (SEI) Layer**

- **SEI Decomposition**

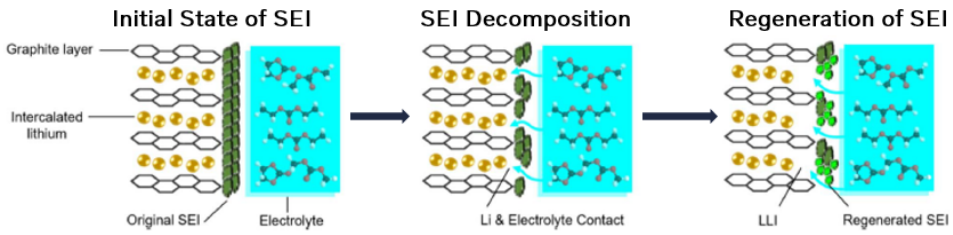

Figure 2.5: SEI layer decomposition and regeneration at High temperature [10]

The above figure 2.5 represents the structural changes occurring in the SEI layer during the process of Thermal runaway.
In the event of a thermal runaway, the excessive heat generated within the

battery can lead to the decomposition of the SEI layer. Once the temperature rises higher and reaches the decomposition temperature ($Tonset$), The elevated temperature causes the SEI layer to break down, releasing volatile organic compounds and reactive species. This decomposition can occur through several possible reactions, depending on the specific composition of the SEI layer and the prevailing conditions.
The decomposition of the SEI layer contributes to the release of flammable gases and further degradation of the electrolyte. The decomposition products, such as alkyl carbonates, carbon dioxide (CO2), and volatile organic compounds, can be reactive and participate in additional chemical reactions. These reactions can generate more heat and increase the severity of thermal runaway. This heat generation can be calculated using the Arrhenius Equation. This equation provides the normalized concentration of SEI and activation energy values.

- **SEI Regeneration**
  The decomposition of the SEI layer can have further reactions and heat generation, While the SEI layer may degrade during thermal runaway, in certain situations, it might also undergo partial regeneration to some extent. This regeneration can be attributed to the presence of certain electrolyte additives or stabilizing agents within the battery. These additives can react with the degraded components of the SEI layer and form a new protective layer on the electrode surfaces. The regeneration of the SEI layer during thermal runaway is not a complete restoration of its original state but rather a partial regeneration. It can provide temporary protection by preventing direct contact between the electrode materials and the electrolyte. However, this partial regeneration is insufficient to fully halt or prevent the overall thermal runaway process.

2.6.2 Anode + Electrolyte

When the SEI layer degrades, it exposes the active materials of the anode electrodes directly to the electrolyte, removing the protective barrier between them. As a result, the electrode materials come into direct contact with the electrolyte, leading to accelerated side reactions. These side reactions can generate additional heat and release volatile gases, further exacerbating the thermal runaway process. The heat generated by these reactions can increase the temperature within the battery cell. The loss of the SEI layer's protective function can also lead to the formation of metal dendrites or filaments on the electrode surfaces. These dendrites can cause internal short circuits within the battery, accelerating the thermal runaway process and potentially leading to a catastrophic failure such as fire or explosion.
The combination of heat generation, gas release, and internal short circuits can lead to a self-sustaining chain reaction, where the thermal runaway process becomes unstoppable until the battery's energy is fully released.

2.6.3 Seperator breakdown

Although the separator's main function is to prevent direct contact between the electrodes, thus avoiding internal short circuits. As the thermal runaway progresses and the temperature within the battery cell continues to rise, the separator's ability to resist heat becomes compromised. At a certain critical temperature, the separator can start to melt. These lead to major stages of TR, such as

- **Loss of Physical Separation**: As the separator melts, the physical barrier between the positive and negative electrodes is compromised. This can result in direct contact between the electrodes, leading to internal short circuits. These short circuits cause a rapid increase in current flow, further increasing heat generation.
- **Thermal Runaway Escalation**: The loss of the separator's integrity allows for an unrestricted flow of charged particles between the electrodes, accelerating the thermal runaway process. The rapid heat generation and continuous release of gases can lead to a self-sustaining chain reaction, making the thermal runaway uncontrollable.
- **Gas and Pressure Build-Up**: The melting separator can also trap and retain volatile gases generated during the thermal runaway process. As more gases accumulate, pressure builds up within the battery cell, increasing the risk of rupture or explosion.
- **Battery Cell Expansion**: The high temperatures and gas generation can cause the battery cell to expand rapidly. The expansion can lead to physical damage to the cell's components and casing, further escalating the safety risks.

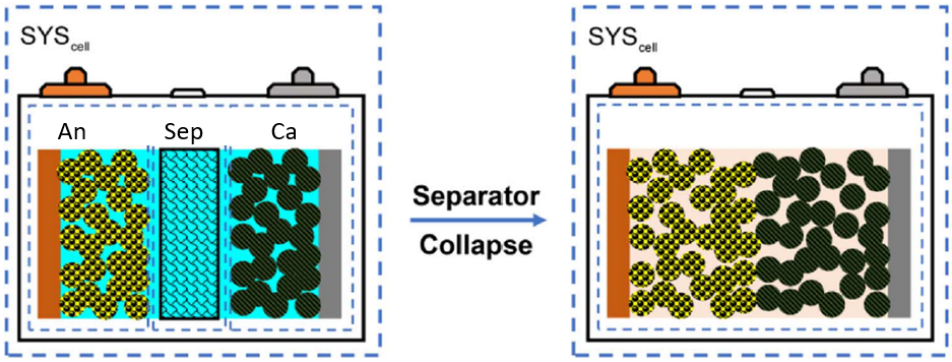

Figure 2.6: Sepertor melting down[10]

2.6.4 Electrolyte decomposition

The increase in temperature begins to affect the integrity of the electrolyte, which consists of organic solvents and lithium salts. At elevated temperatures, the organic solvents in the electrolyte, such as ethylene carbonate (EC) and diethyl carbonate (DEC), start to undergo decomposition. The heat facilitates the breaking of chemical bonds within these solvents, leading to the formation of smaller organic compounds like ethylene compounds and ethane.
The lithium salts can undergo decomposition, resulting in the release of lithium

fluoride (LiF) and other compounds. The decomposition of lithium salts can release fluoride ions, which can further react with the electrode materials or other components in the cell. It includes:

- **Solvent Decomposition**: The organic solvents in the electrolyte, such as ethylene carbonate (EC) and diethyl carbonate (DEC), can decompose into smaller organic compounds like ethylene compounds and ethane. These decomposition reactions are accelerated at high temperatures.
- **Salt Decomposition**: The lithium salts in the electrolyte, such as lithium hexafluorophosphate (LiPF6), can decompose into lithium fluoride (LiF) and other compounds. The decomposition of lithium salts can release fluoride ions, which can further react with the electrode materials.
- **Gas Formation**: The electrolyte decomposition reactions can release volatile gases, such as carbon dioxide (CO2) and other organic compounds. The buildup of these gases can lead to increased pressure within the battery cell.
- **Generation of Reactive Species**: The decomposition of the electrolyte can produce reactive species like radicals, which can participate in additional chemical reactions and further exacerbate the thermal runaway process.

2.6.5 Safety Venting

The temperature and gas generation within the battery cell increases rapidly due to the breakdown of the solid electrolyte interface (SEI) layer, separator melting, and electrolyte decomposition. As a result, the pressure inside the battery cell rises significantly. The build-up of pressure is a critical safety concern because it can lead to cell rupture or explosion. At this stage, the safety venting process comes into play as a crucial safety feature.
When the internal pressure reaches a certain threshold due to the continuous heat and gas generation, the safety venting mechanism is activated. The pressure-activated valve or venting port on the battery cell's casing opens, providing a controlled pathway for the release of gases. There are two stages of gas venting,

- **First Venting(Cell Rupture)** As mentioned above, as the pressure builds up in the battery and exceeds the threshold, the pressure-activated valve placed on the battery's cell casing ruptures and gas flows through it. The first gas venting process helps prevent excessive pressure accumulation within the cell. This controlled gas release relieves the stress on the battery cell's components, reducing the risk of physical damage to the cell and its surroundings. In some cases, only the first venting phase is observed during the thermal runaway test. It is a crucial safety feature that helps prevent catastrophic cell failure during the early stages of thermal runaway. To ensure battery safety during abnormal conditions, modern battery designs implement various safety measures, including gas venting, thermal management, separator and electrolyte selection, and temperature monitoring, all working together to minimize the impact of thermal runaway events.
- **Venting During Thermal Runaway** When the heat generation due to thermal runaway is at high rates it triggers the gases formed during first venting to combust and combustion reactions take place.

2.6.6 Anode & Cathode reactions

After the stage of electrolyte decomposition and separator breakdown stage, there would be no protective layer to avoid contact between the anode and cathode. In this stage, the anode and cathode come in contact and rapid oxidation/reduction reactions are observed during the triggering process. The rapid oxidation-reduction reaction resembles the reaction between the fuel and oxygen in a combustion reaction[10]. It is difficult to capture the exact reactions during this stage because of its complexity and the heat release rate is rapid. The oxidation-reduction reaction is thought to be triggered by "chemical-crosstalk" with the migration of oxide particles over the separator, complicating matters further. This stage triggers an internal short circuit with an increase in current flow, generating additional heat and gas release.

2.6.7 Internal short Circuit & Electrolyte burning

After all the heat generated by each stage of thermal runaway, sums up to the highest temperature and triggers an internal short circuit, and a large amount of current flows through the short-circuited path, bypassing the normal electrical circuit. This uncontrolled current flow generates significant heat, further increasing the temperature inside the battery cell.
This leads to the burning of electrolytes and the combustion of gases that are produced during the venting process, leading to the battery's catastrophic failure and posing hazards to the surrounding environment and users.

2.6.8 Measurement techniques

There are several experimental measurement techniques used to test and study battery thermal runaway.

- **Accelerating Rate Calorimetry (ARC)**

Figure 2.7: ARC Setup image [12]

Accelerating Rate Calorimetry (ARC) serves as a valuable tool for investigating the thermal characteristics of LIB cells. The instrument offers data regarding the thermal behaviour of cell components as well as the thermal hazards of the entire cell. Furthermore, the analysis conducted using ARC enables the collection of valuable data concerning activation energy and thermal kinetic

parameters. ARC operates within an adiabatic environment, simulating the scenario where the heat produced by the sample is utilized to heat the sample itself. As a result, temperature changes occur due to exothermic reactions within the cell, leading to self-heating of the cell.[11] ARC offers information about temperature and pressure changes in the sample and can contain a variety of substances, including high explosives, liquids, and solids. The experimental setup consists of a blast-proof chamber housing a calorimeter assembly. The calorimeter assembly includes three sensors on the top, side, and bottom, each equipped with heaters and thermocouples. Inside the calorimeter, there is a container known as the canister, where the sample is placed, and thermocouples are attached to the sample to measure its temperature [13]. As the temperature rises, the sample undergoes a series of chemical and physical reactions, including electrolyte decomposition and electrode oxidation. These reactions generate heat, and the calorimeter records and monitors the heat flow from the sample throughout the entire process.
The collected heat flow data is examined and studied by researchers. Through this analysis, they can identify the rate at which heat is released, calculate the total amount of heat generated, and pinpoint the temperature at which exothermic reactions take place. This valuable information allows them to assess the seriousness of thermal runaways and better understand the potential outcomes and consequences of such events.
The knowledge acquired through ARC experiments assists in creating battery designs that prioritize safety, choosing suitable materials, and implementing efficient safety protocols to prevent or control thermal runaway incidents.

- **Gas Chromatography-Mass Spectrometry (GC-MS)**
  It is a strong method for analyzing the gases released during battery thermal runaway experiments. When a battery experiences thermal runaway, different gases are produced due to chemical reactions happening inside the cell. GC-MS helps researchers identify and understand these gases, providing crucial information about the reactions taking place and their potential impact on battery safety. The gas chromatograph works by separating the various components of the gas mixture based on their unique chemical properties and sizes of molecules. As the gas components move through a chromatographic column, they travel at different rates, resulting in their distinct separation [14]. These separated gas components leave the chromatographic column, they enter the mass spectrometer. The mass spectrometer identifies and measures the mass and charge of each gas component. Researchers can analyze the chromatogram and identify the different gases present in the sample based on their unique mass spectra.

2.7 GT-SUITE

GT-SUITE is a simulation tool that could be used to create advanced models. More libraries could be used to create system-level models conduct sensitivity analysis of test cases and conduct root cause investigation.

3
Previous work

In this chapter, the research literatures that are relevant to this thesis topic is discussed.

- **TR concept and Review**: With the continuous improvement and rapid increase of electric vehicles, there is a growing need to provide safer and more reliable electric technologies. Research is being conducted on Li-ion batteries. Especially to mitigate battery thermal runaway. Xuning Feng[9] provides the overall review of a battery thermal runaway concept and provides case study results of actual vehicle accidents caused by battery thermal runaway. Different kinds of battery abuses that lead to TR and mitigation research work are explained. Wang[15] explains basic concepts of TR and thermal equations used for heat release and other chemical reactions in the process.
- **Experimental Analysis**: Hoelle[16] Experimental testing of prismatic cells of different capacities was conducted in abuse behaviour and TR behaviour was studied. The tests were conducted both at the module level and cell level and depicted that cell capacity and Battery SOC play a vital role in the TR reaction rate and mass of vented gas. Xuning Feng [10] have conducted TR experiments in ARC and have explained about mechanisms involved.
- **Modeling and Simulation**: The modeling approach of battery TR is well explained with models, equations, and data analysis results by Dongsheng Ren [17]. This journal presents about kinetic analysis of cell components and the models are validated using DSC testing Each TR stage is modeled using Matlab & Simulink. RISE[18][19] 3-D finite element modeling of Battery TR is explained in this journal and is validated by actual test results and developed a model using GT-Suite & Autolion.
- **Venting gas experiments**: Detailed explanation and modeling of gas venting during thermal runaway have been explained in these journals, [20] [21] [22]. The models are validated based on the tear-down of cell data. Vented gas compositions are measured using spectroscopy and the calculation of mass lost is presented.

4

Methodology

In this chapter, the modeling of battery thermal runaway and analysis will be explained. There will be two models explained the first model explains heat generation rate and TR stages concentration rates and the second one explains the venting gas modeling and calculation of total venting gas.

4.1 Literature References

The models are majorly based on these papers,

- Coupled Electrochemical-Thermal Failure Model [10]: In this paper, the methodology to develop electrochemical models of the battery cell and thermal model to capture heat generation by each TR stage is very well explained. The developed model was validated with experimental data on concentration rates. Calculation of activation energy of all chemical reactions during TR was referred from this journal. Decomposition & regeneration of SEI modeling and values were analyzed.
- Thermal runaway of commercial 18650 Li-ion Cells [20]: Experimental testing of overcharging abuse of Li-on cells is conducted in this journal. Two types of cell chemistries are used for the analysis (i.e. NCA & LFP). Complete details of the cell are collected from cell tear-down. Using gas spectroscopy the details of gas venting and battery TR are analysed. Chemical reactions and calculation formulas are referred from this journal. Modeling of the gas venting approach is referred to from [20] and [21]. The experimental results, mass fraction values, and temperature window and analysis were considered for calculations.

4.2 Modelling

In this section modelling of battery cell thermal runaway is explained,

- As mentioned in section 2.6 each TR stage has a different contribution to heat generation and reaction rates. The modeling of TR consists of a combination of the electrochemical model and thermal model. The electrochemical model provides the chemical reactions and electrical characteristics of the battery cell and the thermal model provides the heat generation rates and temperature range.

4.2.1 Electro-Chemical Model

The modeling technique for defining electrical and chemical characteristics involved in TR mechanisms is referred from [10].
The open circuit voltage is measured using the difference between cathode potential and anode potential. The OCV is measured due to the voltage drop that is caused by ohmic potential loss which is caused by the higher temperature leading to entropy change. The model voltage is calculated as indicated in the Eq 4.1

$$ModelVoltage : V_m = U_C - U_A - IR_c + (T - T_r)\frac{dU}{dT} \tag{4.1}$$

Where U_C and U_A are the potentials of the cathode and anode which are measured in the half-cell experiments. I represent the current in the circuit and for discharge condition, it is around 5A. R_c is the average ohmic resistance of the cell. T and T_r are the temperature conditions that are defined during the battery operating conditions, $T_r = 25°C$ initial temperature of the battery cell. The entropy value (dU/dT) at a higher temperature of the cell during OCV testing is around -0.0001V. The potential of electrodes changes concerning battery SOC and this OCV test is conducted before conducting Tr tests in the ARC experiment setup. The OCV values indicate the normal operating conditions of the battery cell test sample that could be used for further analysis.

Battery cell decomposition model
In this section, each stage of battery cell decomposition's reaction rate calculation is explained. The mechanisms having complex kinetics inside the cell are calculated using the Arrhenius Equation [23] which helps to calculate the reaction rates of chemical reactions concerning temperature and constants considered in the experiments.

$$K = Aexp(\frac{-E_A}{RT}) \tag{4.2}$$

where,

- k = rate constant
- A = Frequency factor or Pre-exponential factor (It indicates the frequency of collisions between reactant molecules at a standard concentration.)
- E_A = Activation energy (is the minimum energy needed for the reaction to occur. To fit this into the equation, it has to be expressed in joules per mole.)
- R = Gas constant 8.314 J .mol-1 .k-1
- T = Temperature

1. **SEI decomposition**
   As the temperature increases in the battery and when the temperature reaches the onset temperature of SEI, the decomposition of SEI starts, and the reaction rate is calculated as shown in Eq 4.3

$$SEI_{Decomp} = A_{SEI}c_{SEI}exp(-\frac{E_{a,SEI}}{R^0T}) \tag{4.3}$$

The SEI layer starts to decompose in Li-ion cells from the range (of 85°C to 90°C). c_{SEI} represents the normalized concentration of SEI.

2. **Reactions at Anode:**
   When the SEI layer decomposes, the intercalated lithium ions try to interact with electrolytes and generate heat from the reactions. These reactions also yield an SEI layer in battery cell "formation" cycles. The reaction rate between Li-ions and electrolyte is calculated in Equation 4.4,

$$An_{Decomp} = A_{An} c_{An} exp(-\frac{E_{a,An}}{R^0 T}) exp(-\frac{C_{SEI}}{C_{refSEI}}) \tag{4.4}$$

   These reactions take place when the temperature reaches the onset temperature of the anode (i.e. when $T_{AN}>$ 95°c). The onset temperature varies for different materials used in anode electrodes. The reaction rate of this stage also depends on the thickness of the SEI layer formed. If the SEI layer is thicker the reaction would take place in slow rates and vice versa. To compensate this factor exp(- C_{SEI}/C_{refSEI}) is added in the equation. Where C_{SEI} indicates the value of the normalized factor of the current SEI layer and C_{refSEI} indicates the value of the normalized factor of the initial SEI layer.

3. **SEI layer regeneration**
   As described in section 2.6.1, due to the presence of electrolyte additives and SEI leftover new layer of SEI is formed. This regeneration of SEI would cause a loss of li-ions in the anode inventory. This directly affects the calculation of the reaction rate and heat generation at the anode stage 4.4 and certain values need to be added considering these factors. Newly formed SEI would also lead to an increase the cell resistance. Further, an increase in the temperature would lead to the separator melting stage.

4. **Separator melting & Electrolyte vaporization**
   As the temperature reaches 150°C the PE (Polyethylene Membrane) base of the separator starts to melt and the resistance of the separator increases [9]. In detail, the theory of separator breakdown can be referred from the previous section 2.6.3. When temperature increases up to 200°c the separator becomes thinner and finally leads to breakdown. This can be seen in the figure 4.1.

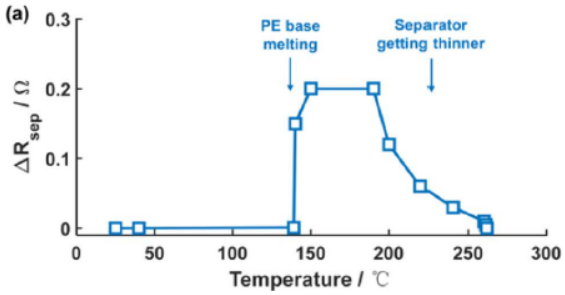

Figure 4.1: Resistance growth during separator breakdown stage. [10]

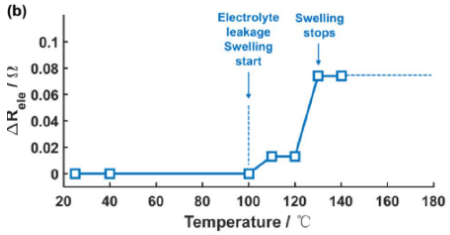

Figure 4.2: Resistance growth during electrolyte vaporization stage. [10]

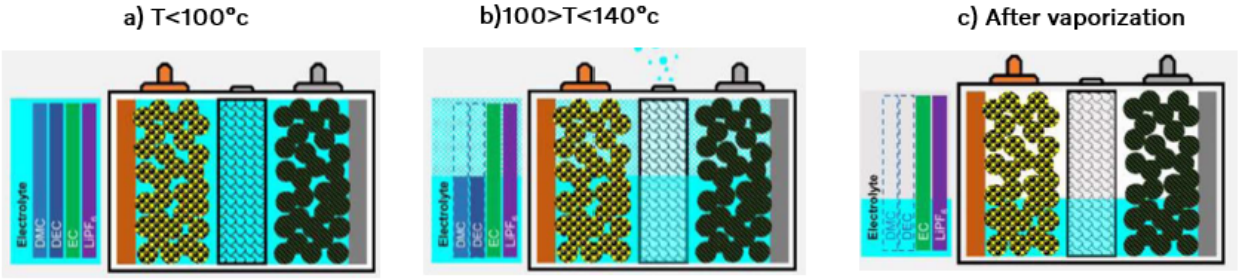

Figure 4.3: Electrolyte solvents vaporization with respect temperature. [10]

The electrolyte also starts to vaporize as resistance increases and at a temperature of 100°c DMC (Dimethyl carbonate). The boiling point of DMC is around 90°c and the other solvents in electrolytes also start to vaporize and would lead to interactions between anode and cathode electrodes. These temperature profiles also vary concerning solvents present in electrolytes. Battery cells swell when the process of solvent vaporization starts.

5. **Loss of active materials in electrodes (LAE)**
   Due to the leakage of electrolyte solvents, the active materials of the anode and cathode electrodes start to decrease. The capacity of electrodes (Q_{An} & Q_{Ca}) decreases and this can be formulated to calculate the reaction rates. The initial capacity of anode and cathode active materials in a normal battery cell is represented as Q_{intAn} & Q_{intCa}.

$$Q_{An} = c_{LAE,An} Q_{intAn} \tag{4.5}$$

$$Q_{Ca} = c_{LAE,Ca} Q_{intCa} \tag{4.6}$$

$$c_{LAE,1} = c_{LAE,An} [c_{LAE,An} = c_{SEI}] \tag{4.7}$$

$$LAE = -A_{LAE} (c_{LAE,2})^2 exp(\frac{E_{a,LAE}}{R^0 T}) \tag{4.8}$$

In equation 4.8 A_{LAE} indicates the value of the pre-exponential factor of electrodes and $c_{LAE,2}$ indicates the value of the normalized factor of cathode electrodes during interaction with anode active material. The normalized factor, $c_{LAE,2}$ can only be utilized when the electrolyte is in the gas stage and the

onset temperature of the electrolyte.

6. **Internal Short Circuit (ISC)**
The final stage of the model leads to an internal short circuit caused by anode and cathode interaction. At temperatures above 300°c, an internal short circuit is triggered and heat is generated.

$$I = (\frac{V_m}{R_{SC}}) \tag{4.9}$$

where V_m and R_{SC} are the voltage of the model and resistance in the cell during a short circuit. The heat generated can be calculated as shown in the equation 4.10

$$Q_{ISC} = I^2(R_{cell} + R_{SC}) \tag{4.10}$$

The calculated values of reactions for the above TR stages are mentioned below.

z	Δh_z/J · g^{-1}	m_z/g	$c_{z,0}$	$n_{z,1}$
SEI	150*	100.58	0.15	1
anode	1714	100.58	1	1
separator	-190	17.6	1	1
cathode,1	77	179.12	0.999	1
cathode,2	84	179.12	0.999	1
electrolyte	800	108	1	1
z	$T_{\text{onset},z}$ /°C	A_z/s^{-1}	$E_{a,z}$/J · mol-1	$\frac{dc_z^g}{dt}$
SEI	50	1.667×10^{15}	1.3508×10^5	$K_{\text{SEI}}^g \cdot \frac{dc_{\text{anode}}^d}{dt}$
anode	50	0.038* (T<260) 5 (T>260)	3.3×10^4	0
separator	120	1.5×10^{50}	4.2×10^5	0
cathode,1	180	1.75×10^9	1.1495×10^5	0
cathode,2	220	1.077×10^{12}	1.5888×10^5	0
electrolyte	120*	1.5×10^{13}*	1.5×10^5*	0

Figure 4.4: Table representing the Reaction kinetics for the components of the lithium-ion cell [10]

4.2.2 Thermal model calculating heat generation

This model calculates the heat generated from each mechanism of TR and is finally coupled with the electro-chemical model in GT-Suite.

$$\rho_c C_{p_c}(\frac{dT}{dt}) = Q_{irr} + Q_{rev} + Q_{abuse} - Q_{discharge}[25] \tag{4.11}$$

where,
ρ_c = Density of the battery cell
C_{p_c} = Specific heat capacity of the cell (1100J .kg-1 .K-1)
Q_{irr} = Irreversible heat generation
Q_{rev} = Reversible heat generation
Q_{abuse} = Heat generated by all the abuse reactions
$Q_{discharge}$ = Heat rejected to environment

Q_{irr} is the heat generated due to the difference between the potential of open-circuit and the battery cell operating potential. this includes the ohmic resistances and mass transfer heat [24]. Q_{rev} is the heat generated by the electrode reactions and battery cell entropy changes. $Q_{discharge}$ is equal to zero in this model because there would be an adiabatic environment in the ARC test setup.

$$Q_{abuse} = Q_{chem} + Q_{ISC} \tag{4.12}$$

$$Q_{chem} = Q_{SEI} + Q_{An} + Q_{Seperator} + Q_{Ele} + Q_{An+Ca} \tag{4.13}$$

where,
Q_{SEI} = heat generated by SEI decomposition
Q_{An} = heat generated by decomposition at anode
$Q_{Seperator}$ = heat generated during separator breakdown
Q_{Ele} = heat generated by electrolyte decomposition

Q_{An+Ca} is the total heat generated during the interaction between anode and cathode active material. The decomposition of the cathode has two separator reactions which would be indicated as **Cathode 1** and **Cathode 2**. Cathode 1 is the condition where cathode material starts to decompose during the electrolyte burning and Cathode 2 represents the interaction of cathode and anode electrode. The reaction between the cathode and anode is the typhoid oxidation-reduction reaction formed by the "chemical-crosstalk" [10] [25]. This reaction indicates the combustion reaction for battery fire during TR. The heat calculation formula for all the chemical reactions is represented in a general format.

$$Q_{chem} = \Delta h_{chem} m_{cell} (\frac{dc_{chem}}{dt}) \tag{4.14}$$

where,
Δh_{chem} = Specific enthalpy of chemical reactions (J/kg)
m_{cell} = mass of the battery cell(g)
c_{chem} = normalised factor chemical reactions

4.3 Modelling in GT-Suite

As mentioned in section 2.7, considering the modelling tools and libraries battery TR model was developed in GT-SUITE.
The modeling approach was to replicate the ARC testing methodology in GT-SUITE using its library. Two models are created, one is related to simulation TR mechanisms and capturing heat generation values and the other one is related to gas venting simulations and mass loss calculation model.

4.3.1 Heat and TR mechanisms Model

The main methodology involved in developing this model is combining the electro-chemical model and thermal model equations to capture the reaction rates of TR stages.

- **Battery Specifications used in the model**

Battery Cell Specifications	Values
Cell Chemistry	NMC(Nickel Manganese& Cobalt) 811
Cell Format	Prismatic
Anode material	Graphite
Anode foil	Copper
Cathode Foil	Aluminum
Separator Layer	Polymeric Membrane
Electrolyte solvents	DMC:DEC:EC=1:1:1
Cell mass	720g
OCV at 100% SOC	4.3V

- **Description of model and templates used**
  The overview concept model is represented as shown in figure 4.5. The testing battery cell is placed inside a reactor with an inert environment. There would be a flow inlet and outlet with a flow of inter gas to the chamber. The battery cell has no internal load to test TR. An external heat source is utilized to trigger the cell. The external heat control unit is used to control the heat load to the cell according to the temperature inside the cell. The chemical connector is a chemical solver that would capture and implement the electro-chemical model equations to the battery cell. Chemical reactions, energy values, entropy values, and reference temperature data will be implemented in the chemical reaction block. When the cell is triggered to TR, the reaction rates and temperature data are sensed by the chemical connector solver and sent to heat sensing and concentration sensing sensors which will be seen on heat generation and concentration monitors. In detail points about each component will be explained below.

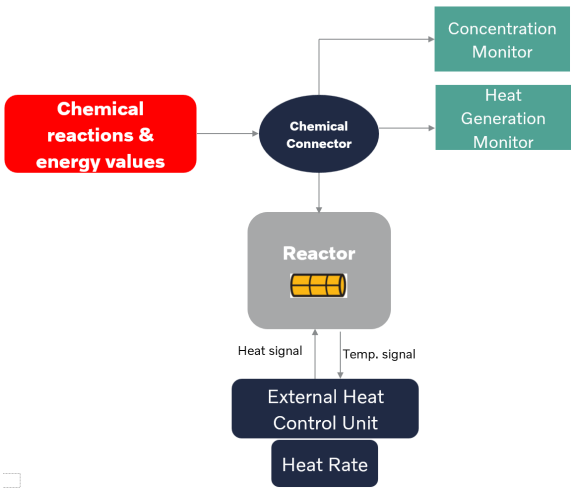

Figure 4.5: Schematic diagram of TR model developed in GT-Suite

1. **External Heat Control unit:**
   In this modeling approach, the battery cell is triggered by an external heat source. The test scenario in this model considers the overcharge abuse condition of battery TR. The external heat control unit mainly consists of three parts signal generator, math equation, and integrator templates.

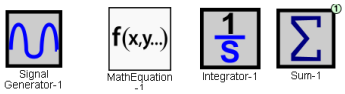

Figure 4.6: Templates used in external heat control unit

Signal Generator templates are used to generate heat input. There are two heat inputs to the control unit, one is the battery cell triggering heat rate input which starts from 60°c and the other is an extra heat rate that needs to be added considering the stage of TR in the battery cell. This cross-talk heat is the external heat that is generated by cathode and anode reactions in the end stage of TR. This extra heat rate is added to the control unit if the temperature is above 350°c. The math equation templates are used to perform mathematical calculations using input values and math equations. The heating rate limiter in the control unit mainly controls the heat rate input to the model. As mentioned, if the cell temperature is above 60°c, the heat rate input is sent into the main heat sum template. The Crosstalk heat is limited by using a crosstalk heat switch which adds extra heat when the temperature is above 350°c. The integrator senses the temperature of the battery cell using the temperature sensor and calculates the amount of heat rate that needs to be added. The final crosstalk heat rate limiter performs math calculations considering the temperature value and TR stages and provides the heat rate to the final sum template. All these templates are connected using the link function. The summation heat is implemented further into the AutLion battery cell using the heat rate actuator connector which connects the signal from the control unit to multi-physics library parts.

2. **AutoLion**
   The AutoLion template is a representation of John Newman's "Pseudo 2D" (P2D) electro-chemical model designed for Lithium-ion (Li-ion) batteries. This model depicts the electro-chemical reactions within a Li-ion cell and makes predictions regarding terminal voltage, current, power, heat dissipation, and Lithium content across the cell. John Newman's P2D model achieves this by breaking down the governing equations of the Lithium-ion cell into discrete units using the finite control volume method. The Cathode, Separator, and Anode components are divided in the "thickness" dimension. Within each finite control volume of the Cathode and Separator, there is a spherical representation of active material. These representations are divided into consistent volumes in the radial direction [26]. The interface of the AutoLion template is shown in the below figure 4.7. The template is an option to modify the physical values and electrical values of the battery cell. Physical attributes were considered from NMC prismatic cells as mentioned in the table 4.3.1.

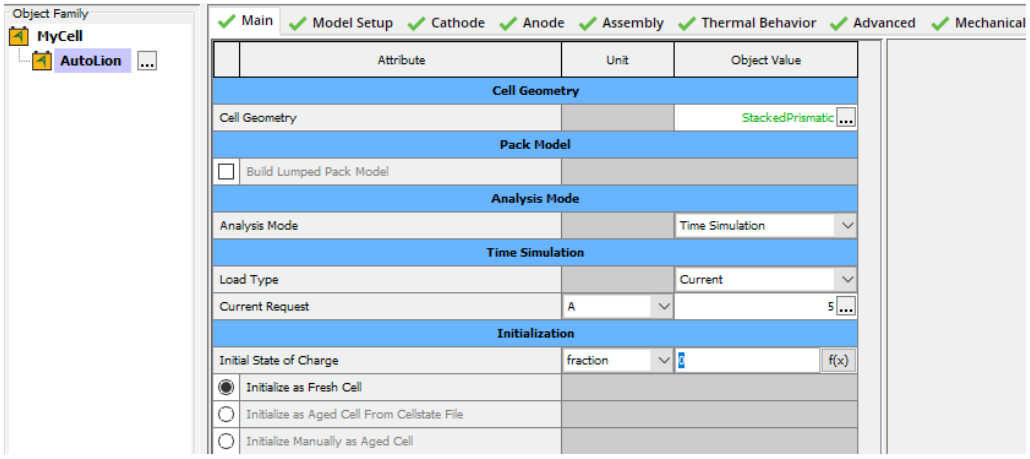

Figure 4.7: Template interface and details of Autolion in GT-SUITE

The electro-chemical model which was described in section 4.2.1 is implemented in this template. Specific mass values of TR reactions are referred from experimental data and the heat values are obtained from the calculations in thermal model 4.2.2. Activation energy and pre-exponential factor values are referred from the literature [10]. The concentration expressions column provides the sequence and the phenomenons to be considered with respect temperature of a particular TR stage. These concentration expressions are defined in the figure 4.8.

Cell Component Mass	Specific Heat	Reactants	Products	Pre-exponent Multiplier	Activation Temperature or	Concentration Expressions
g	J/kg				J/mol	
100.58	150000.0	metasei	product	1.0	0.0	G(8)
100.58	17140...	anodesolvent	product	1.0	33000.0	{anodesolvent}*G(2)*G(7)*G(9)
17.6	-19000...	sep	product	1.5E50	420000.0	{sep}*G(3)
108.0	800000.0	ec	product	1.5E13	150000.0	{ec}*G(4)
179.12	77000.0	cath1	product	1.75E9	114950.0	{cath1}*(1-{cath1})*G(5)
179.12	84000.0	cath2	product	1.077E12	158880.0	{cath2}*(1-{cath2})*G(6)

Figure 4.8: Implementing of reactions kinetics parameters in AutoLion

The above data implements the thermal runaway stage sequence according to their respective temperature window. The specific heat rate values are considered from the heat calculation of different TR phenomenons. The Reactants and products columns represent the chemical reactions of each TR stage and the products that will be formed during the process. The values of the pre-exponent multiplier are the chemical solver values that are used to specify the rate of reactions which are referred from [10]. In order to capture the heat rate and concentration rate of TR phenomenons, reactions are switched on based on the initial temperature of each stage. This temperature scale can be seen in the figure 4.9. The specific conditions in TR stages such as SEI regeneration, cathode-anode reaction, and anode reactions with binder and electrolyte are equated in general function expression. These pre-defined functions are used in chemical solvers to solve the reaction with respect to its activation energy and specific heat.

Optional Description of General Functions	General Function Expressions G(i)
SEI reaction switch	if(T>50+273,1,0)
Anode reaction switch	if(T>50+273,1,0)
Separator reaction switch	if(T>120+273,1,0)
Electrolyte reaction switch	if(T>120+273,1,0)
Cathode 1 reaction switch	if(T>180+273,1,0)
Cathode 2 reaction switch	if(T>220+273,1,0)
Pre-exponent multiplier ...	if(T<260+273,0.038,5)
SEI formation and rege...	if(T>50+273,1,0)*(1.667e15*exp(-135080/8.314/T)*{metasei}-6*if(T<26...
Anode reaction slow down	2exp(-{metasei}/0.15)

Figure 4.9: Temperature window data of each TR stage

4.3.2 Gas Venting model

In this model, the gas venting mechanisms and mass loss calculations modeling are explained. The heat and gas generation processes within a Li-ion battery cell are difficult to model because of the chemical reactions involved. It needs to be modeled using complex reactions and thermal runaway conditions.
The gas generation mechanisms in Li-ion battery cells involve multiple chemical reactions and the products are in different stages which makes it complicated to capture all the gas phenomenons. This model is developed to capture the gases produced during the thermal abuse reactions hence it is only suitable for analyzing the gases at the thermal runaway stage of battery cells. Some of the assumptions made for calculations of gas species are mentioned below:

1. All the thermal abuse reactions of thermal runaways are summed to one model and used for heat generation and to capture temperature windows. The heat generated is considered to be at its peak.
2. The rate of gas generation is proportional to the rate of thermal abuse reactions. [21].
3. The solid particulates ejected during the TR process are not considered for mass calculations.
4. Battery SOC is considered to be more than 100%.

- **Calculation equations:**
  The generalized equation for calculating the masses of gas species is given below,

$$Cell_{mass} = xGas_{Volatiles} + (1 - x)Cell_{remains} \tag{4.15}$$

  where $Cell_{mass}$ is the initial cell mass (g) before conducting the TR simulation. $Gas_{Volatiles}$ & $Cell_{remains}$ are the different gas volatiles and the remaining solid particles(g) in the battery cell. x is the mass fraction of the cell that turns into gas volatiles.
  The rate of abuse reaction ($d\alpha/dt$) and heat generation are expressed as follows [21]:

$$d\alpha/dt = -A_{ab}(\alpha)^m exp(-E_{ab}/RT)exp(-B_{ab}(\alpha)) \tag{4.16}$$

$$S_{heat} = Q_{Spc}d\alpha/dt \tag{4.17}$$

  where S_{heat} is the source term for heat generation value. Q_{Spec} is the specific heat value(KJ/m^3),α is the degree of reaction progress of TR stages, A_{ab} is

the reaction rate parameter $(1/s)$ and E_{ab} is the energy value which is fitted into the equation 4.16 and B_{ab} is a non-dimensional parameter as per the reference[21]. The volumetric rate of gas generation due to devolatilization is calculated using the below equation,

$$S_v = xW_{Spcv}(d\alpha/dt) \tag{4.18}$$

W_{Spcv} is the initial specific content of the cell material (initial cell mass/cell volume)(g/m^3). x represents the mass fraction of the cell that turns into gas volatiles. We also want to capture the mass fraction of each gas species:

$$S_{m,gas} = Y_i S_v \tag{4.19}$$

Y_i represents the mass fraction of particular gas species that would be sensed during TR. $S_{m,gas}$ is the source term for each gaseous species.

- **Gas Species:**
  In this model, only the main gas compositions of venting gas are captured and considered for calculations. The six main gas compositions considered are, $(H_2,\ CO_2,\ CO,\ CH_4,\ C_2H_4,\ C_2H_6)$. The main chemical reactions that involve these gas species during the TR stage are shown below and The kinetic rate of these gas reactions is considered from the literature's [27] & [28].

Reactions	Kinetic Rate [kmol m^{-3} s^{-1}]
$H_2 + 0.5O_2 \rightarrow H_2O$	$1 \times 10^{11} \exp\left(-\frac{10000}{T_g}\right)[H_2]^1[O_2]^{0.5}$
$CH_4 + 1.5O_2 \rightarrow CO + 2H_2O$	$5.0 \times 10^{11} \exp\left(-\frac{24055}{T_g}\right)[CH_4]^{0.7}[O_2]^{0.8}$
$C_2H_4 + 2O_2 \rightarrow 2CO + 2H_2O$	$1.125 \times 10^{10} \exp\left(-\frac{15000}{T_g}\right)[C_2H_4]^{0.1}[O_2]^{1.65}$
$C_2H_6 + 2.5O_2 \rightarrow 2CO + 3H_2O$	$6.18 \times 10^{9} \exp\left(-\frac{15000}{T_g}\right)[C_2H_6]^{0.1}[O_2]^{1.65}$
$CO + 0.5O_2 \rightarrow CO_2$	$2.239 \times 10^{12} \exp\left(-\frac{20450}{T_g}\right)[CO]^{1}[O_2]^{0.25}[H_2O]^{0.5}$

Figure 4.10: Kinetic Rate of Gas Combustion Reactions (numerators in the exponential have the unit of K).

- **Model in GT-SUITE:**

  The schematic diagram of the gas model is represented as shown in the figure 4.12. The model mainly consists of 3 major sections: reactor, heat control & cell control units, and gas sensing unit. The Li-ion battery cell is placed inside the battery cell and the reactor has an inlet that provides the intake of inert gas and an outlet that is used to capture the venting gases. Inert gas is used to provide inert ambient conditions inside the reactor so that there are no other by-products formed from the ambient environment, this way we could capture the exact gas species. The heat control unit functions on the same principle as explained in the section 1 but it is connected to the cell control unit which is a thermal node in GT-SUITE that would operate the TR tiger mechanisms and other battery boundary conditions would be implemented in it. As the battery cell reaches the onset temperature the thermal runaway

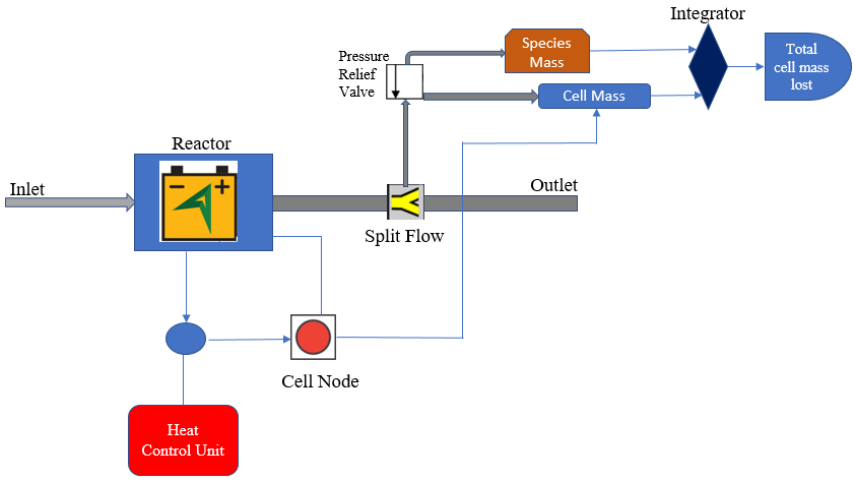

Figure 4.11: Schematic diagram of the gas model

occurs. The combustion gases vent out and reactions occur. The gases vented pass through the outlet flow pipe which consists of a split flow pipe that helps to deviate the gases to the analysis sector. As the pressure is observed in the split flow using the pressure relief valve the gases are sensed and passed to the species mass-capturing block. The remaining solid particulates or other gas particulates are sent to the cell mass block. Inside the species mass block, each gas species is sensed and sent to an integrator where the mass fraction values are integrated concerning initial cell mass and finally indicate the total cell masses lost using TR.

The model setup in GT-SUITE is represented below.
The major changes compared to the heat model 4.3.1 using thermal node and gas species reactor volume templates.
The heat rate and cell thermal properties are entered into the thermal node. The thermal node also gives the data of cell mass which is used to calculate the remaining cell mass. The pressure relief valve opens at 10 bar and the gas species data is sent from the reactor volume template which discrete the vented gas into different gas components and provides the details of all the gas species mass.
Gas species values and reactions are implemented in the AutoLion template. Modeling parameters and TR conditions remain the same as described in the heat model. The gas species fluid objects are defined using gas fluid libraries with an initial fraction has zero. In the reaction section, extra reactants and products are added considering the combustion gas reactions.

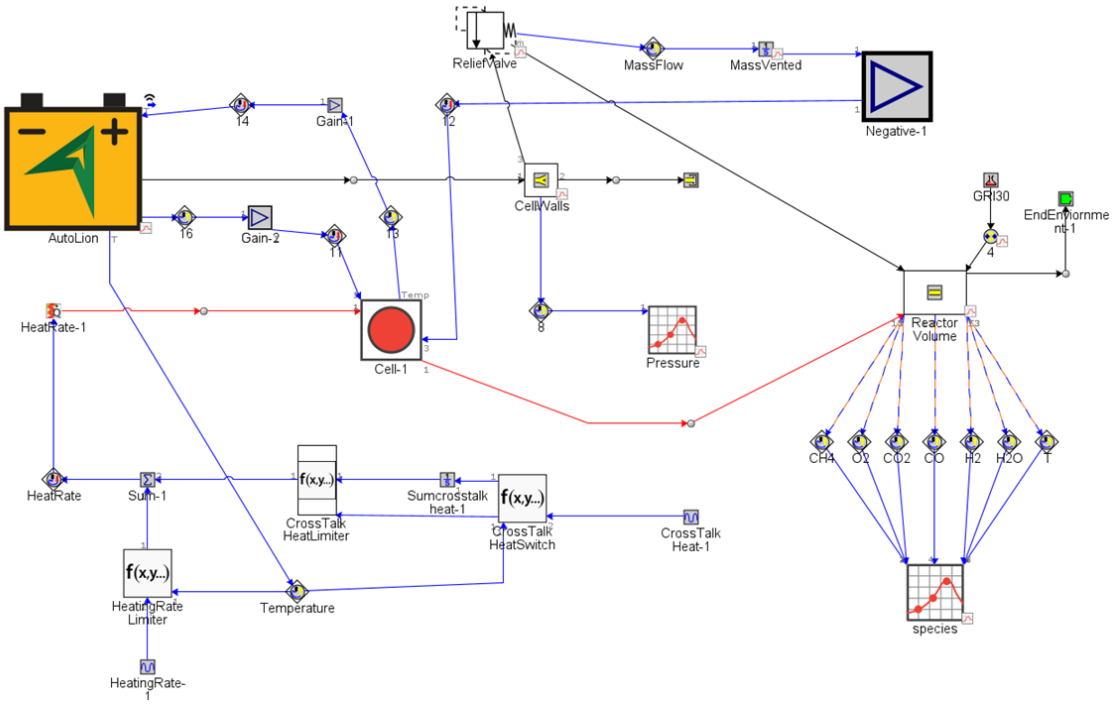

Figure 4.12: Gas model in GT-SUITE

5
Results

5.1 Heat Model

This section explains the results obtained from the Heat model 4.3.1. Explains the sequence map of thermal runaway stages and plot of heat generation.

5.1.1 Heat Generation plots

- **Heat Generated by TR mechanisms:** Figure 5.1, indicates the heat value curves of $Q_{reactions}$ & Ca+An reactions. The dotted purple line represents the heat behavior of the Cathode+Anode oxidation-reduction reaction. Total heat generated by the TR stage 2.6.6 alone equals 30KW. As we come across the theory behind the reaction rate involved between cathode and anode is rapid and generates more heat. These reactions take place at higher temperatures and involve complex chemical reactions. The green curve represents the heat curve of $Q_{reactions}$ which is the sum of heat generated by all the other TR mechanism's reactions which is equal to 44KW. These curves are represented in a single plot to indicate the value of heat that is generated by Ca+An reactions when compared to other TR mechanisms.

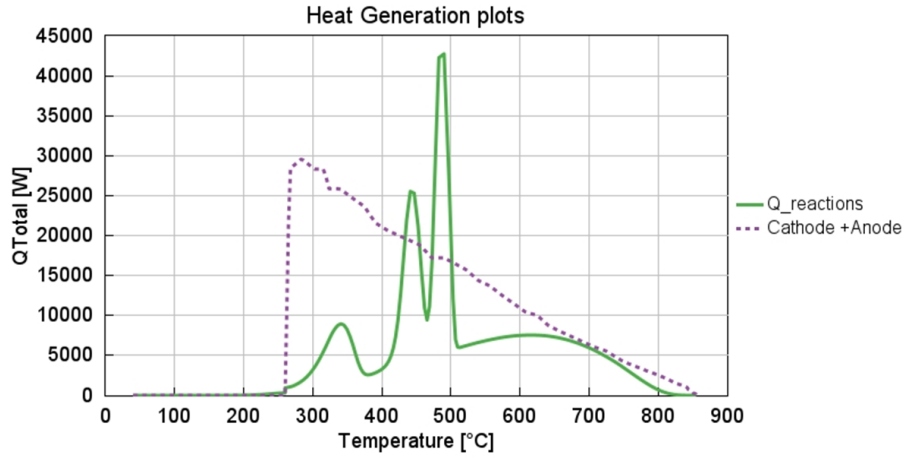

Figure 5.1: Heat generation plots of $Q_{reactions}$ & Cathode+Anode reaction VS T

- Figure 5.2 represents the heat curves of all the TR mechanisms concerning temperature. The green curve in Figure 5.1 is discrete into multiple reactions in this figure. As we can observe the heat generation curves from different

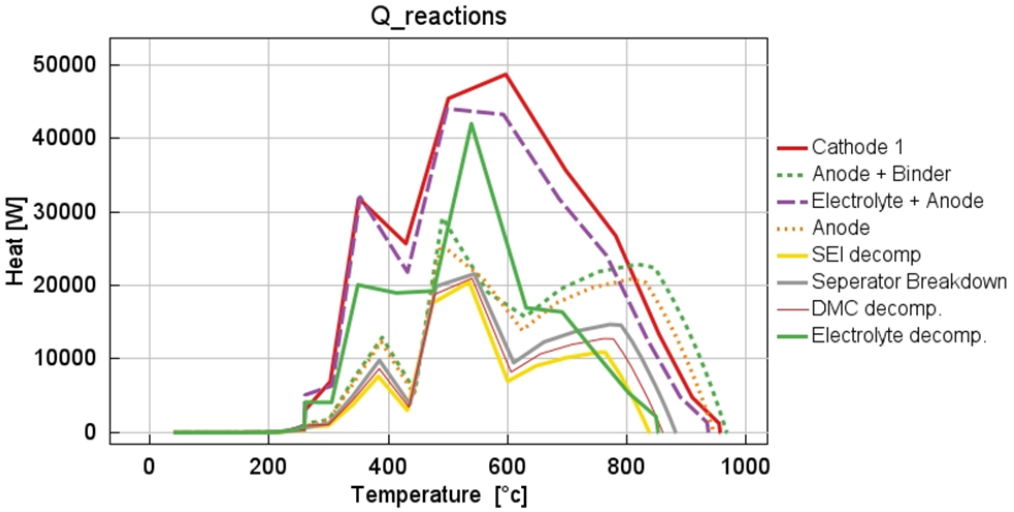

Figure 5.2: Heat Generation plots of all other TR mechanisms VS T

mechanisms increase as the TR stages involve more reactions and cell components. This heat generation also depends on the composition percentage of components involved in TR. As we can see in the plot, the stages that have less composition in battery cells have less heat generation. SEI and separator are less compared to other components. DMC (Dimethyl carbonate) is one of the salt content in electrolytes it starts in the early stage to produce heat because its boiling point is at 100°C. When an anode would be decomposing there would be different stages involved such as Anode + Binder, Anode + Electrolyte, and anode. The model captures heat generated by reactions of the anode this detailed modeling would be very much useful by seeing the differences in heat generated by each stage of anode compositions. Cathode 1 is considered as part of cathode decomposition where only the heat generated by cathode active material is considered. It generates the highest heat among the reactions because amount of cathode inventory present in the electrode.

- **Model Validation**

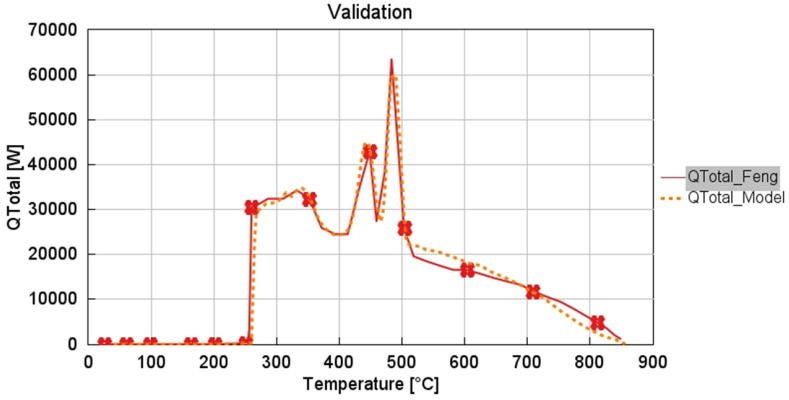

Figure 5.3: Validation of heat plots with Feng paper [10]

Figure 5.3 represents the results of validation of the total heat generation curve of the model with the Feng model. The dotted orange curve illustrates the total heat generation of the model which is the sum of $Q_{recations}$ curve and the Ca+An curve in the figure 5.1. The total heat generated for the model equals 60 KW and the heat generated from the Feng model is around 60 KW which can be seen from the red curve in the figure.

5.1.2 Concentration of reactions and sequence map

The concentration rates captured in TR stages are as shown in figure 5.4. Kinetic rates calculated in the section 4.2.1 are used in the model to capture this data. The concentration fractions are plotted against temperature where the maximum TR temperature reaches up to 950°C and the species concentrations fall from 1 to 0. The reaction curves have occurred in a sequence indicating the TR stages. Where TR initiates from 90°C with SEI decomposition there could be a small rise in SEI concentration around 110°C This is because of SEI layer regeneration during reactions between the anode and electrolyte. Anode reactions are seen to be having reactions until 900°C this is because of its reaction rates and active material inventory. Other TR stage reactions occur in sequences with respect to their temperature window.

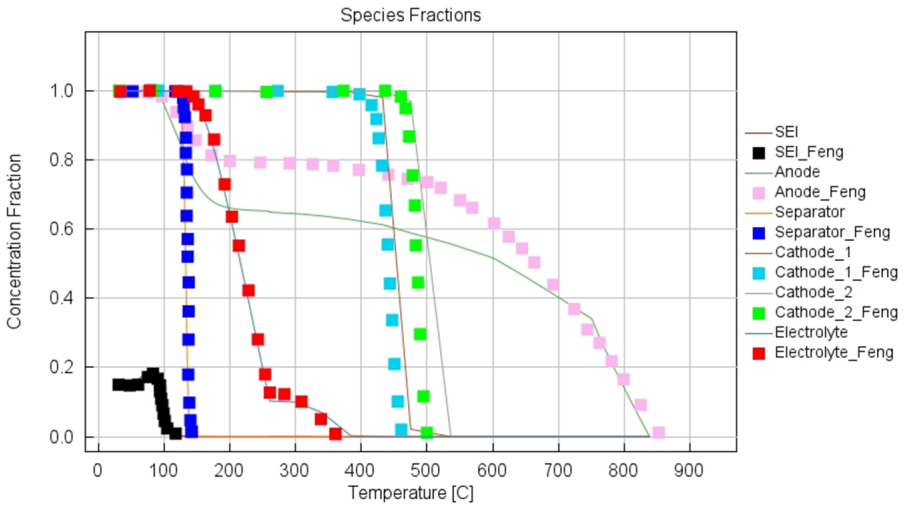

Figure 5.4: Normalised concentration of TR reactions

5.2 Gas Model

The major result of the gas model indicates the mass fraction of the vented gases and the possible sources for it. As discussed in section 4.3.2, the model mainly captures 6 gas species and the data is listed in the figure 5.5. These gas species are from the NMC Li-ion battery cell at SOC > 100% which is tested in an inert gas environment. Methane mass fraction is highest compared to other gas species at high temperatures. The oxygen released during reactions also contributes to the

Gas	Possible Gas Sources	Mass (g) in%	Temperature Range
H2 Hydrogen	Reaction of binder with Li ions (at anode side)	2.67%	@ T>230 ° C
CO2 carbon-dioxide	SEI & Electrolyte (at cathode side)	23%	@ T>280 ° C
CO Carbon monoxide	Reduction of CO2 with intercalated Li at anode	20%	@ T>300 ° C
CH4 methane	Reduction of electrolyte to Li carbonate (in the presence of H2)	42%	@ T 280° C
C2H4 Ethylene	Produced by the reduction of electrolyte at the Li anode	6%	@ T 230° C
C2H6 Ethane	Reduction of DMC at anode	6.33%	@ T 210 ° C

Figure 5.5: Table of vented gas during TR

combustion of these gas species which is not captured in this model. CO_2 and CO are also the highest formed gases during the battery cell thermal runaway. Other gases such as H_2, C_2H_4 and C_2H_6 are produced in less amount. The total gases produced during TR are sensed to be around 56g and the other solid particulates and residuals are sensed to be around 245g. Out of 720g of total battery cell mass, 42% is lost during battery thermal runaway of which 18% is from the venting gas process and the remaining is from the solid particulates. These values when validated with different experimental results indicate deviations of values with respect to the mass fraction of gas species.

6

Conclusion & Future Work

6.1 Conclusion

The modelling approach for battery cell thermal runaway has enabled us to understand and analyse cell-level behaviours during high temperatures and abuse conditions. The electro-chemical and thermal models developed can be used to study and analyse the reactions that are involved in battery thermal runaway. These models could be used as a baseline for developing models for other commercial Li-ion chemistry battery cells by modifying the temperature and chemical substances with respect to battery cells. In-detail sequencing and data of thermal runaway phenomenons could be utilised for module-level and pack-level simulations by referring to the temperature values and mass of gases that will be venting out. The results from the heat model indicate the importance of analysing and understanding the mechanisms of the Cathode-Anode oxidation-reduction reaction which contributes to the major part of heat generation during TR. The gas venting model that is developed only provides the result of the second venting gas process and the mass fraction values are not accurate when validated with experimental data. The possible gas source data can be used to validate the amount of gases produced in the second venting gas process. The accurate way to capture the gas value is by considering the initial gas formation during the initial stages of TR and integrating it with calculations of combustion gases, in this way, the mass of gas vented could be calculated in the right way and would be useful to validate experimental results. As this approach considers overcharging abuse conditions, it is very well understood from the results and thermal models that battery SOC plays a major role in TR.

6.2 Future Work

From the understanding of the complexity of battery thermal runaway mechanisms, there are a lot of things to be developed at the cell level to use its results in system-level simulations. Heat generation and gas venting phenomena need to be integrated into a single model which would not affect each other's results. Developing models for other thermal runaway triggering abuse conditions such as (mechanical, thermal, ageing, etc). Battery SOC data points should be considered and included in the modelling of battery thermal runaway because, at different SOC levels, the TR mechanisms are different and help also to create critical points for battery operations. The gas venting modelling approach should try to capture the source of combustion gases and should be analysed with respect to battery SOC.

Bibliography

[1] Kai Wai Wong, Wan Ki Chow, "Principle for the Working of the Lithium-Ion Battery", Journal of Modern Physics, DOI:10.4236/jmp.2020.1111107

[2] Casimir, Anix, et al. "Silicon-based anodes for lithium-ion batteries: Effectiveness of materials synthesis and electrode preparation." Nano Energy 27 (2016): 359-376.

[3] Patranika, Tamara. "Investigations of the Thermal Runaway Process of a Fluorine-Free Electrolyte Li-Ion Battery Cell." 2021.

[4] Hui Cheng and Joseph G. et al. "Recent progress of advanced anode materials of lithium-ion batteries", Journal of Energy Chemistry, 57 (2021), 2095-4956.

[5] CHINTABATTUNI RAJARATNAM, "Understanding Different Battery Chemistry", 2022.

[6] Jeffrey W. Fergus, "Recent developments in cathode materials for lithium ion batteries", Journal of Power Sources, 195 (2010), 0378-7753.

[7] Murashko, Kirill, "Thermal modelling of commercial lithium-ion batteries", DOI:10.13140/RG.2.1.3930.0723, 2016.

[8] Yamauchi, Takashi, et al. "Development of a simulator for both property and safety of a lithium secondary battery." Journal of power sources 136.1 (2004): 99-107.

[9] Feng, Xuning, et al. "Thermal runaway mechanism of lithium ion battery for electric vehicles: A review." Energy storage materials 10 (2018): 246-267.

[10] Feng, Xuning, et al. "A coupled electrochemical-thermal failure model for predicting the thermal runaway behavior of lithium-ion batteries." Journal of The Electrochemical Society 165.16 (2018): A3748.

[11] TAMARA PATRANIKA, "Investigations of the Thermal Runaway Process of a Fluorine-Free Electrolyte Li-Ion Battery Cell", KTH Publications, 2021.

[12] Stainless Steel White EV-Accelerating Rate Calorimeter.

[13] Mohamad Syazarudin, et al. "Characterisation of thermal runaway behaviour of cylindrical lithium-ion battery using Accelerating Rate Calorimeter and oven heating", Case Studies in Thermal Engineering 28 (2021): 101474.

[14] F. Moya, et al. "Gas spectroscopy and temperature measurement by coherent Raman anti-stokes scattering", Optics Communications, 13 (1975), 0030-4018.

[15] Wang, Qingsong, et al. "Thermal runaway caused fire and explosion of lithium ion battery." Journal of power sources 208 (2012): 210-224.

[16] Hoelle, S., et al. "Analysis on thermal runaway behavior of prismatic lithium-ion batteries with autoclave calorimetry." Journal of The Electrochemical Society 168.12 (2021): 120515.

[17] Ren, Dongsheng, et al. "Model-based thermal runaway prediction of lithium-ion batteries from kinetics analysis of cell components." Applied energy 228 (2018): 633-644.
[18] Huang, Chen, et al. "Modelling thermal runaway initiation and propagation for batteries in dwellings to evaluate tenability conditions." (2022).
[19] Willstrand, Ola, et al. "Impact of different Li-ion cell test conditions on thermal runaway characteristics and gas release measurements." Journal of Energy Storage 68 (2023): 107785.
[20] Golubkov, Andrey and Scheikl, Sebastian and Planteu, Rene and Voitic, Gernot and Wiltsche, Helmar and Stangl, Christoph and Fauler, Gisela and Thaler, Alexander and Hacker, Viktor "Thermal runaway of commercial 18650 Li-ion batteries with LFP and NCA cathodes - Impact of state of charge and overcharge", RSC Adv., 2015.
[21] Kim, Jinyong, et al. "Modeling cell venting and gas-phase reactions in 18650 lithium ion batteries during thermal runaway." Journal of Power Sources 489 (2021): 229496.
[22] Abbott, Katie C., et al. "Comprehensive gas analysis of a 21700 Li (Ni0. 8Co0. 1Mn0. 1O2) cell using mass spectrometry." Journal of Power Sources 539 (2022): 231585.
[23] Mohamad, Ahmad Azmin. "Absorbency and conductivity of quasi-solid-state polymer electrolytes for dye-sensitized solar cells: A characterization review." Journal of Power Sources 329 (2016): 57-71.
[24] Diaz, Laura Bravo, et al. "Measuring irreversible heat generation in lithium-ion batteries: An experimental methodology." Journal of The Electrochemical Society 169.3 (2022): 030523.
[25] Jindal, Puneet, Banoth Sravan Kumar, and Jishnu Bhattacharya. "Coupled electrochemical-abuse-heat-transfer model to predict thermal runaway propagation and mitigation strategy for an EV battery module." Journal of Energy Storage 39 (2021): 102619.
[26] Description of GT- AutoLion template is given in the website and more details are provided in the software.
[27] Westbrook, Charles K., and Frederick L. Dryer. "Simplified reaction mechanisms for the oxidation of hydrocarbon fuels in flames." Combustion science and technology 27.1-2 (1981): 31-43.
[28] Magnussen, Bjørn F., and Bjørn H. Hjertager. "On mathematical modeling of turbulent combustion with special emphasis on soot formation and combustion." Symposium (international) on Combustion. Vol. 16. No. 1. Elsevier, 1977.

DEPARTMENT OF SOME SUBJECT OR TECHNOLOGY
CHALMERS UNIVERSITY OF TECHNOLOGY
Gothenburg, Sweden
www.chalmers.se

CHALMERS
UNIVERSITY OF TECHNOLOGY